Spatial inequalities of COVID-19 mortality rate in relation to socioeconomic and environmental factors across England

Abstract:

In this study, we aimed to examine spatial inequalities of COVID-19 mortality rate in relation to spatial inequalities of socioeconomic and environmental factors across England. Specifically, we first explored spatial patterns of COVID-19 mortality rate in comparison to non-COVID-19 mortality rate. Subsequently, we established models to investigate contributions of socioeconomic and environmental factors to spatial variations of COVID-19 mortality rate across England (N = 317). Two newly developed specifications of spatial regression models were established successfully to estimate COVID-19 mortality rate (R^2 = 0.49 and R^2 = 0.793). The level of spatial inequalities of COVID-19 mortality is higher than that of non-COVID-19 mortality in England. Although global spatial association of COVID-19 mortality and non-COVID-19 mortality is positive, local spatial association of COVID-19 mortality and non-COVID-19 mortality is negative in some areas. Expectedly, hospital accessibility is negatively related to COVID-19 mortality rate. Percent of Asians, percent of Blacks, and unemployment rate are positively related to COVID-19 mortality rate. More importantly, relative humidity is negatively related to COVID-19 mortality rate. Moreover, amongst the spatial models estimated, the 'random effects specification of eigenvector spatial filtering model' outperforms the 'matrix exponential spatial specification of spatial autoregressive model'.

Keywords: COVID-19 mortality; Spatial disparities; Matrix exponential spatial specification model; Eigenvector spatial filtering model; Socioeconomic disadvantage

1. Introduction

COVID-19 infection and mortality are gaining increasingly attentions from both policymakers and researchers. Owing to privacy protection individual-level COVID-19 data are not publicly available, aggregate COVID-19 data plays a key role in COVID-19 research. Recently, aggregate-level geocoded or georeferenced COVID-19 mortality data in some countries or regions have been released as well. Therefore, geovisualisation and spatiotemporal analysis of COVID-19 mortality rate are performable. As empirical evidence on the association of socioeconomic and environmental factors and a variety of health outcomes have been found, we could speculate that spatial variations of COVID-19 mortality rate might be associated with spatial variations of socioeconomic and environmental characteristics (e.g., Ji et al., 2020; Yao et al., 2020; Coker et al., 2020) and this speculation could be empirically validated by geographically aggregated COVID-19 death data.

In this study, we aimed to examine spatial inequalities of COVID-19 mortality rate in relation to spatial inequalities of socioeconomic and environmental factors. Specifically, we first explored spatial patterns of COVID-19 mortality rate in comparison to non-COVID-19 mortality rate. Subsequently, we modelled spatial variations of COVID-19 mortality rate from local-scale socioeconomic and environmental characteristics. Empirically, we used the England-wide COVID-19 mortality rate data aggregately collected from March to May of 2020. These 3 months are experiencing most fast-growing deaths duo to COVID-19 in England. England is chosen as the empirical study area because 1) England is one of the most serious countries in Europe according to either number of COVID-19 cases or number of COVID-19 deaths; 2) local-scale COVID-19 mortality data, socioeconomic data, and environmental data across England are publicly available.

This study can offer more evidence on the associations of COVID-19 mortality rate, socioeconomic and environmental factors. An understanding of spatial inequalities of COVID-

19 mortality rate in relation to socioeconomic and environmental characteristics can inform policymakers to prioritise areas with a lower socioeconomic status or a lower environmental quality (e.g., air quality) in response to a second wave of COVID-19 or alike crises. Compared to the previous studies, this study is the first one taking account of both socioeconomic factors and environmental factors simultaneously in explaining spatial variations of COVID-19 mortality rate; and the first one focusing on spatial variations of COVID-19 mortality rate in relation to socioeconomic factors and environmental factors across England.

As the regression models are applied to geospatial data in this study, spatial regression models are highly recommended. Spatial autocorrelation is likely to exist in the residuals of non-spatial regression models (e.g., ordinary least squares models) applied to geospatial data. Presence of spatially autocorrelated residuals means individual observations are not completely independent, thereby violating the assumption of observation independence in regression models. In this case, we should replace nonspatial models with spatial regression models since spatial regression models, like spatial autoregressive models, are developed to reduce the adverse impact of auto-correlation in regression residuals. Therefore, in this study, we selected two typical spatial regression models: spatial autoregressive model and eigenvector spatial filtering model as the former is the most widely used one (e.g., Chi and Zhu, 2008; Lin 2010) and the latter is likely to perform best (e.g., Chun, 2014; Helbich and Jokar Arsanjani, 2015). More specifically, the matrix exponential spatial specification model and fast random effects eigenvector spatial filtering model are selected to estimate models in this study. The ‘matrix exponential spatial specification’ is one of the best specifications in spatial autoregressive models (LeSage and Pace 2009); whilst the ‘random effects specification’ is one of the new and effective specifications in eigenvector spatial filtering models (Murakami and Griffith 2015). Compared with conventional specifications of spatial autoregressive models, the ‘matrix exponential spatial specification’ has advantages on computational efficiency and

interpretation (e.g., generation of R^2) (LeSage and Pace, 2007), and the 'random effects specification' is likely to better explain the spatial variations with a higher value of R^2 or a lower value of Akaike information criterion (Murakami and Griffith 2015; Murakami and Griffith 2019). Furthermore, we will compare the performance of the models estimated and determine which models are more appropriate.

This study can offer more evidence on the associations of COVID-19 mortality rate, socioeconomic and environmental factors. Particularly, this study empirically reveals that spatial variations of COVID-19 mortality rate are mainly attributable to spatial variations of socioeconomic and environmental characteristics across England. Healthcare resource allocation should prioritise some areas around Sunderland, Liverpool, and Birmingham since those areas are hotspots of COVID-19 mortality rate and non-COVID-19 mortality rate but have a lower level of access to hospital.

2. Literature review

Health inequalities exist among different socioeconomic groups since socioeconomic status (SES) reportedly influences health outcomes (e.g., Nobles et al 2013; Präg et al 2016; Kosidou et al 2011). A number of studies had offered empirical evidence on the association of socioeconomic factors and human health, including physical health (e.g., Nobles et al 2013; Präg et al 2016) and mental health (e.g., Nobles et al 2013; Präg et al 2016; Kosidou et al 2011). Adverse socioeconomic factors such as poverty, unemployment, and occupational risks are likely to cause negative health consequences. Socioeconomically disadvantaged people are likely to live a less healthy life, including lower access to healthcare, healthy food, or recreational facilities, a lower level of physical activity, a higher level of exposure to alcohol and/or tobacco, less knowledge of health maintenance, or a lower level of self-discipline. In general, people with a lower socioeconomic position are more likely to suffer from health

problems than those with a higher socioeconomic position. Apart from socioeconomic factors, environmental factors are found to influence health outcomes (e.g., Hoek et al., 2013; Beelen et al., 2014; Wheeler et al. 2015; Lelieveld et al., 2015; Di et al., 2017). For instance, increased mortality due to different causes is reportedly associated with air pollution exposure (Hoek et al., 2013; Beelen et al., 2014; Lelieveld et al., 2015; Di et al., 2017), road traffic noise exposure (Halonen et al., 2015; Héritier et al., 2017), temperature (Gasparrini et al., 2015; Guo et al., 2014), and humidity (Barreca and Shimshack, 2012; Ou et al., 2014).

Some recent studies had performed interesting research using georeferenced COVID-19 case data though those data had been aggregated to a variety of geographic units (e.g., state/province, county/town/city, etc.) before being released. To search for COVID-19 incidence hotspots, some researchers detected spatiotemporal clusters of COVID-19 cases across United States (Hohl et al., 2020; Desjardins et al., 2020). To understand socioeconomic and environmental effects, some scholars modelled spatial variations of COVID-19 incidence rate from socioeconomic and environmental factors in China (e.g., Huang et al., 2020; Guliyev 2020), United States (e.g., Mollalo et al., 2020), and Africa (e.g., Adekunle et al., 2020). Besides, some city-wide researches had been conducted as well (e.g., Cordes and Castro, 2020). Moreover, some scholars modelled the dynamic spread of COVID-19 through travel patterns of people (Zheng et al., 2020; Gatto et al., 2020; Velásquez and Lara, 2020; Danon et al., 2020; Pujari and Shekatkar, 2020).

Although not being discussed as much as COVID-19 infection or spread, COVID-19 mortality and its associations with socioeconomic and environmental characteristics have been discussed in a few studies. On the one hand, socio-economically advantaged communities are likely to have a higher risk of COVID-19 mortality. A recent study of primary COVID-19 data in England uncovers that Black, Asian and minority ethnic groups in England are at increased

risk of death from COVID-19 (Aldridge et al., 2020). Similarly, another recent study reveals that substantial racial/ethnic disparities are observed in COVID-19 case fatality and mortality with Blacks/African Americans disproportionately affected across the United States (Holmes et al., 2020). In the United States, black people are being admitted to hospital and dying in disproportionate numbers from the covid-19 pandemic (Dyer, 2020). A systematic review of recent literature concludes that Black, Asian, and Minority Ethnic (BAME) individuals are at an increased risk of worse clinical outcomes from COVID-19 (Pan et al., 2020). Moreover, unemployment and poverty are reported to be an important factor in determining COVID-19 mortality rates in France (Goutte et al., 2020). More specifically, focusing on a densely populated region of France, Goutte et al. (2020) documented evidence that higher economic "precariousness indicators" such as unemployment and poverty rates, lack of formal education and housing are important factors in determining COVID-19 mortality rates. Besides, access to healthcare is likely to play a key role in affecting COVID-19 mortality rate. Spatial variations in healthcare resource availability and accessibility might partly explain spatial disparities variations in COVID-19 mortality rate across China (Ji et al., 2020). On the other hand, environmental characteristics (e.g., air quality, temperature range, and humidity) are likely to affect COVID-19 mortality. For instance, a recent study found positive associations between particulate matter pollution ($PM_{2.5}$ and PM_{10}) and COVID-19 case fatality rate (CFR) in Chinese cities (Yao et al., 2020). Another study on other Asian cities suggests that there exists a positive correlation between the level of air pollution of a region and the lethality related to COVID-19, indicating air pollution to be an elemental and concealed factor in aggravating the global burden of deaths related to COVID-19 (Gupta et al., 2020). Similarly, a positive association of ambient PM2.5 concentration on excess mortality related to the COVID-19 epidemic was found in Northern Italy (Coker et al., 2020). Effects of temperature variation and humidity on COVID-19 mortality rate were reported as well (Ma et al., 2020). More

specifically, Ma et al. (2020) explored the effects of meteorological factors on COVID-19 mortality in Wuhan, and found that diurnal temperature range is positively associated with daily death counts of COVID-19 while absolute humidity is negatively associated with daily death counts of COVID-19.

3. Materials and methods

3.1 Research data

The mortality data is available for March, April and May in 2020 (https://www.ons.gov.uk/peoplepopulationandcommunity/birthsdeathsandmarriages/deaths/datasets/deathsinvolvingcovid19bylocalareaanddeprivation). The data offer the number of deaths and age-standardised rates by local authority districts (LADs) according to deaths occurring between March and May. Figure 1 maps three-month COVID-19 mortality rate and non-COVID-19 mortality rate across England at the local authority district (LAD) level. Besides, there are 317 LADs constituting England. In Figure 1, grey areas mean areas with no data.

Population by gender and LAD is available for 2019 (https://www.ons.gov.uk/peoplepopulationandcommunity/populationandmigration/populationestimates/datasets/populationestimatesforukenglandandwalesscotlandandnorthernireland), and population by ethnicity and LAD is available for 2017 (https://www.ons.gov.uk/peoplepopulationandcommunity/populationandmigration/populationestimates/adhocs/008781populationdenominatorsbybroadethnicgroupandforwhitebritishlocalauthoritiesinenglandandwales2011to2017). Unemployment rate by LAD is available for 2019 (https://www.ons.gov.uk/employmentandlabourmarket/peoplenotinwork/unemployment/datasets/modelledunemploymentforlocalandunitaryauthoritiesm01/current), and percent of

168 households in poverty by LAD is available for 2014
169 (https://www.ons.gov.uk/peoplepopulationandcommunity/personalandhouseholdfinances/inc
170 omeandwealth/datasets/householdsinpovertyestimatesformiddlelayersuperoutputareasinengla
171 ndandwales). A household is thought to be in poverty if its income is below 60% of the median
172 income before housing costs. Locations of hospitals are available from UK National Health
173 Service (NHS) (https://www.nhs.uk/about-us/nhs-website-datasets/).

174 Since high-resolution $PM_{2.5}$ data and climatic data are not available for 2020, high-resolution
175 $PM_{2.5}$ data and climatic data for 2019 were used. Specifically, Met Office offers 1x1 km
176 gridded monthly relative humidity and air temperature (maximum and minimum) for 2019
177 (Met Office, 2020); whilst Defra offers 1x1 km gridded annual mean $PM_{2.5}$ data for 2019
178 (https://uk-air.defra.gov.uk/data/pcm-data). Air pollution maps at 1x1 km resolution are
179 modelled each year under Defra's Modelling of Ambient Air Quality (MAAQ) contract. These
180 maps are used to provide policy support for Defra and to fulfil the UK's reporting obligations
181 to Europe. The models have been calibrated using monitoring data from the national network
182 sites. Professional monitoring stations installed in monitoring sites are used to observe air
183 quality, humidity, and temperature (see https://uk-air.defra.gov.uk/networks/network-
184 info?view=aurn and https://www.metoffice.gov.uk/public/weather/observation/map). We used
185 the average climatic measures of three months (i.e., March, April and May) in 2019 to represent
186 the climatic measures (i.e., relative humidity and range of air temperature) used in this study.
187 Although monthly high-resolution $PM_{2.5}$ is not available, population-weighted LAD-level
188 annual mean $PM_{2.5}$ is available, and thereby is used to represent the annual mean $PM_{2.5}$ level
189 used in this study. Technically, monthly relative humidity and monthly air temperature were
190 aggregated from grids to LADs. Figure 2 maps population and density of hospital across
191 England at the local authority district (LAD) level in 2019. And, Figure 3 maps annual mean
192 PM2.5 across England at the local authority district (LAD) level in 2019.

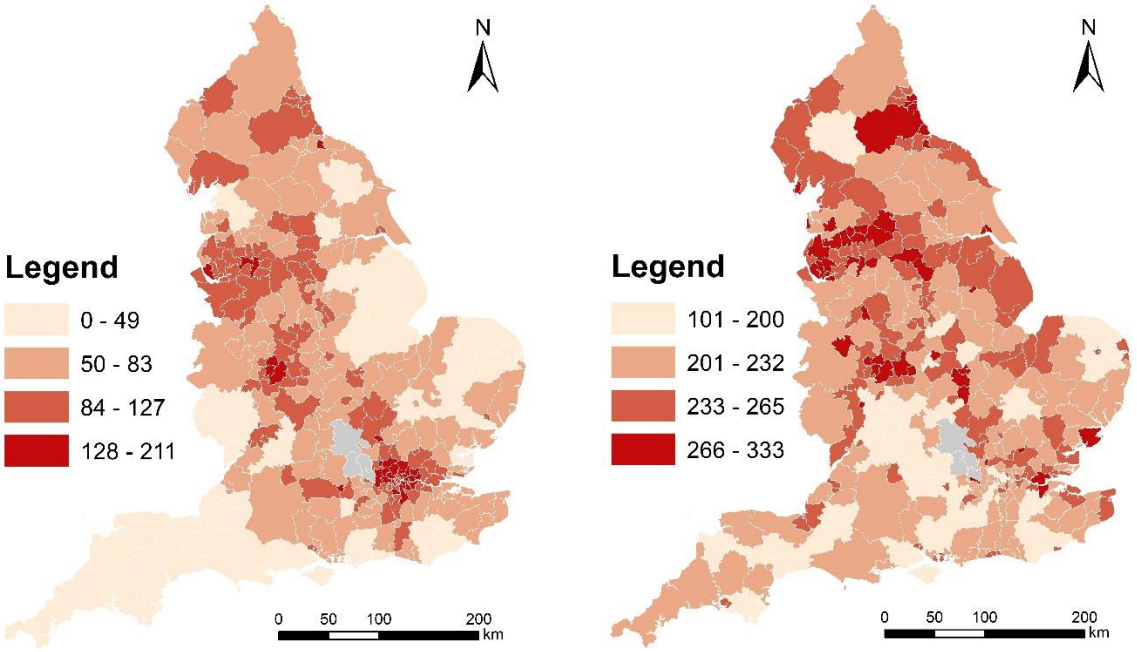

a) COVID-19 mortality rate b) Non-COVID-19 mortality rate

Figure 1. 3-month COVID-19 mortality rate and non-COVID-19 mortality rate across England at the local authority district (LAD) level (March, April, and May 2020) (Data source: ONS)

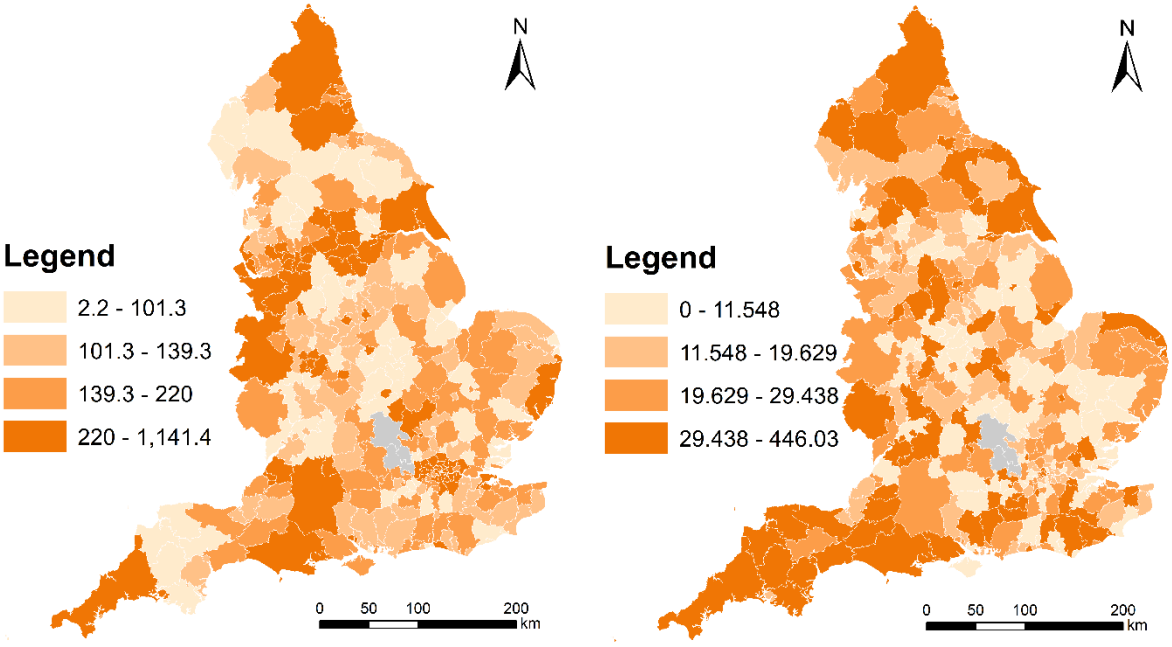

a) Population (unit: 1,000 persons)

b) Density of hospital (unit: number of hospitals per 1,000,000 persons)

Figure 2. population and density of hospital across England at the local authority district (LAD) level in 2019 (Data source: ONS and NHS)

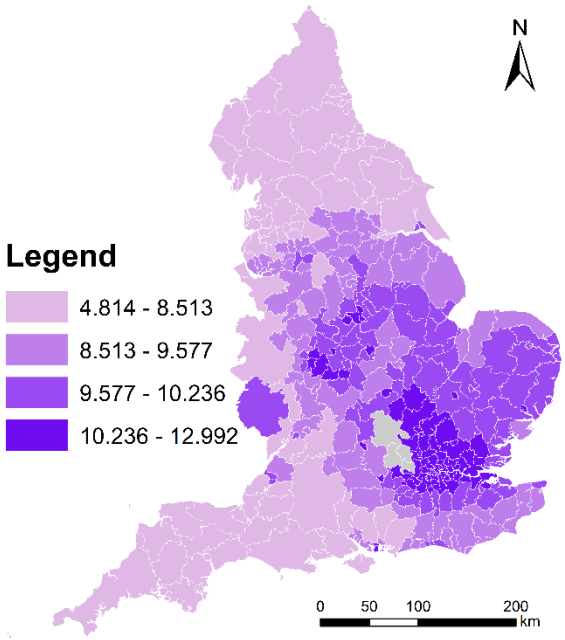

198 **Figure 3.** annual mean $PM_{2.5}$ (unit: ug / m^{-3}) across England at the local authority
199 district (LAD) level in 2019 (Data source: Defra)

200

201 *3.2 Exploring spatial patterns of COVID-19 mortality rate*

202 In this study, we first explored spatial patterns of COVID-19 mortality rate in comparison with
203 non-COVID-19 mortality.

204 3.2.1 Assessing spatial inequalities of COVID-19 mortality and non-COVID-19 mortality

205 In this study, we assessed spatial inequalities of COVID-19 mortality rate and non-COVID-19
206 mortality rate by computing the Gini coefficient (the most commonly used measure of
207 inequality).

208 3.2.2 Exploring spatial association of COVID-19 mortality and non-COVID-19 mortality

209 In this study, we explored spatial association of COVID-19 mortality rate and non-COVID-19
210 mortality rate by using bivariate Moran's *I* test. Specifically, bivariate Moran's *I* test includes
211 global and local ones. The global one is also called "global indicators of spatial association
212 (GISA)", and the local one is also called "local indicators of spatial association (LISA)". The

global and local ones are used to quantify the global and local spatial association between two variables respectively. Specifically, a positive association (a positive Moran's *I* value) means high (low) values of one variable is surrounded by high (low) values of the other variable; whilst a negative association (a negative Moran's *I* value) means high (low) values of one variable is surrounded by low (high) values of the other variable.

3.3 Modelling spatial variations of COVID-19 mortality rate

3.3.1 Model variables

Table 1 lists the variables considered in this study. The response is three-month COVID-19 mortality rate (unit: deaths per 100,000 persons). The explanatory variables include socioeconomic characteristics (i.e., gender, ethnical, income, and employment characteristics), hospital accessibility, and physical environment characteristics (i.e., air pollution, humidity, and temperature measures). The range of air temperature equals the difference of maximum air temperature and minimum air temperature. Particularly, a population-based measure is used to quantify the level of hospital accessibility rather than an area-based one as the response is a population-based one as well. Table 1 also shows the statistical description for all the variables in this study.

There might be still potential bias because all the explanatory variables are measured in 2019 or earlier while the response (COVID-19 mortality rate) is measured in 2020. We made an assumption that spatial variations of socioeconomic and environment characteristics across a country should be consistent between continuous years. For instance, spatial variations of socioeconomic and environment characteristics across England in 2020 should be proportional to those in 2019; likewise, spatial variations of socioeconomic and environment characteristics in 2019 should be proportional to those in 2018 as well. Table 2 lists the correlations of LAD-level explanatory variables and their counterparts in the previous years (Note that P_HIP is not included due to the absence of data in other years). As Table 2 shows, high values of Pearson's

correlation coefficients (R > 0.9) indicate that spatial variations of socioeconomic and environment characteristics in 2019 is highly proportional to those in 2018. Based on the assumption, spatial variations of socioeconomic and environment characteristics in 2020 is likely to be highly proportional to those in 2019 as well. Therefore, we can use spatial variations of socioeconomic and environment characteristics in 2019 or earlier to approximately represent spatial variations of them in 2020.

Table 1. Summary of variables and data sources in this study.

Variable	Full Name	Mean	SD	Year	Source
CMR	3-month COVID-19 mortality rate (unit: deaths per 100,000 persons)	79.4	36.89	2020	ONS
P_F	Percent of females	50.65	0.83	2019	ONS
P_A	Percent of Asians	6.11	8.11	2017	
P_B	Percent of Blacks	2.52	4.65	2017	
P_HIP	Percent of households in poverty	15.84	3.36	2014	
UE_R	Unemployment rate (%)	3.66	1.21	2019	
D_P	Density of population (unit: 1,000 persons per km^2)	1.8	2.64	2019	
D_H	Density of hospital (number of hospitals per 1,000,000 persons)	23.33	27.96	2019	NHS
AM_PM	Annual mean $PM_{2.5}$ (ug / m^{-3})	9.38	1.59	2019	Defra
R_H	3-month mean relative humidity (%)	76.28	1.9	2019	Met Office
R_AT	3-month mean range of air temperature (^oC)	8.97	0.84	2019	

Table 2. Correlations of LAD-level explanatory variables and their counterparts in the previous year or earlier (*N*=317)

Pearson's correlation coefficient	P_F 2018	P_A 2016	P_B 2016	UE_R 2018	D_P 2018	AM_PM 2018	R_H 2018	R_AT 2018
P_F 2019	0.993							
P_A 2017		0.999						
P_B 2017			0.999					
UE_R 2019				0.995				
D_P 2019					0.999			
AM_PM 2019						0.935		
R_H 2019							0.9	
R_AT 2019								0.933

3.3.2 Model selection and estimation

To select and estimate appropraite models, we will first estimate spatial regression models as well as non-spatial regression models, and subsequently check whether spatial regression models can reduce residual spatial autocorrelation in comparion with non-spatial regression models.

Moran's *I*: Testing for spatial dependence:

To test whether there is significant spatial autocorrelation present in regression residuals, we will use the Moran's *I* testing method proposed by Moran (1950). Moran's *I* is widely used to measure the level of spatial autocorrelation between adjacent locations (Moran 1950; Getis and Ord 1992).

Variable selection: the Lasso technique

Lasso (Tibshirani, 1996) performs automatic variable selection and is most likely the preferred method (Friedman 2010; Engebretsen and Bohlin, 2019). In this study, we used Lasso to select explanatory variables and further estimate models to improve model estimation.

Spatial regression models:

If significant spatial autocorrelation is found to exist in the residuals of non-spatial regression models estimated conventionally, we should consider spatial regression models. In this study, we will select two specifications from two types of spatial regression models (i.e., spatial autoregressive and eigenvector spatial filtering) since the former is the most widely used one and the latter is thought to be most high-performance one. Specifically, we will use the matrix exponential spatial specification (MESS) and random effects specification (RES) as specifications in the spatial autoregressive (SAR) models and in eigenvector spatial filtering (ESF) models respectively.

Spatial autoregressive model (MESS-SAR): Among different types of spatial regression models, spatial autoregressive model is the most popular one. A variety of spatial autoregressive (SAR) models have been proposed to remedy residual spatial autocorrelation. Specifically, we choose the matrix exponential spatial specification (MESS) as the specific SAR model in this study since the MESS model has analytical, computational, and interpretive advantages over other SAR models (LeSage and Pace, 2007). Additionally, the MESS-SAR model produces R^2 values which are direct measures of the explanation capacity of the model; whilst conventional spatial regression models do not. The coefficients estimated in the MESS-SAR model are usually similar to those in OLS models, but residual spatial correlation is much lower (LeSage and Pace 2007; LeSage and Pace 2009). The MESS model can be described as follow (LeSage & Pace, 2007; LeSage & Pace, 2009):

"A spatial regression mode can be expressed as

$$Sy = X\beta + \varepsilon \quad (1)$$

where the vector *y* contains *n* observations on the dependent variable, each associated with one region or point in space. The matrix *X* represents an $n \times k$ full column rank matrix of constants which correspond to observations on *k* independent variables for each region. The *n*-element vector ε is distributed as $N(0, \sigma^2 I_n)$. The *k* element vector β is a vector of corresponding parameters, and *S* denotes an $n \times n$ non-singular matrix of constants that may depend on an unknown real, scalar parameter.

The MESS specification replaces the conventional geometric decay of influence from higher-order neighbouring relationships implied by the spatial autoregressive process with an exponential pattern of decay in influence from higher-order neighbouring relationships. Specifically, the MESS model transforms *S* to model spatial dependence among the elements of the vector *y*:

$$S = e^{\propto W} = \sum_{i=0}^{\infty} \frac{\propto^i W^i}{i!} \quad (2)$$

where *W* is an $n \times n$ non-negative matrix with zeros on the diagonal and α represents a scalar real parameter. *W* represents a spatial weight matrix, and $W_{ij} > 0$ indicates that observation *j* is a neighbour of observation *i*. The matrix exponential *S*, along with matrix *W*, imposes a decay of influence for higher-order neighbouring relationships."

Eigenvector spatial filtering model (RES-ESF): Compared to spatial autoregressive models estimated based on parametric estimation methods (e.g., maximum likelihood estimation or Bayesian estimation), eigenvector spatial filtering is computer intensive since it is a nonparametric statistical method which is distribution free without sacrificing too much information in a sample (Tiefelsdorf and Griffith, 2007). Although eigenvector spatial filtering

(ESF) models are computationally demanding, they are likely to outperform spatial autoregressive models in the applications of urban and regional studies, ecological studies, and so on (Murakami and Griffith 2019). Furthermore, a random effects specification of ESF (RES-ESF) had been developed because of its usefulness for spatial dependence analysis considering spatial confounding (Murakami and Griffith 2015). RES-ESF model is found to outperform conventional ESF model (Murakami and Griffith 2015; Murakami and Griffith 2019). Besides, the RES-ESF model can produce R^2 values as well.

The eigenvector spatial filtering (ESF) is also called Moran's eigenvector-based spatial regression approach in regional science (Griffith 2003), and ESF with a small number of eigenvectors (i.e., small L) can greatly reduce model misspecification errors and increases model accuracy (Murakami and Griffith, 2019). The ESF model is presented as follows (Chun et al., 2016):

"ESF utilizes the spectral decomposition of a transformed spatial weights matrix, **C**. The spectral decomposition of matrix **MCM** (where $\mathbf{M} = (\mathbf{I} - \mathbf{1}\mathbf{1}^{\mathrm{T}})/n$ and **1** is a vector of ones) produces a set of n eigenvalues and their corresponding eigenvectors:

$$\mathbf{MCM} = \mathbf{E}\boldsymbol{\Lambda}\mathbf{E}^{-1} = \mathbf{E}\boldsymbol{\Lambda}\mathbf{E}^{\mathbf{T}} \tag{3}$$

where $\boldsymbol{\Lambda}$ is a diagonal matrix whose diagonal elements are the n eigenvalues $\boldsymbol{\lambda} = (\lambda_1, \lambda_2, \ldots, \lambda_n)$ ordered from the largest value to the smallest value, and $\mathbf{E} = (\mathbf{e}_1, \mathbf{e}_2, \ldots, \mathbf{e}_n)$ represents the n corresponding eigenvectors. As an output of the spectral decomposition, the eigenvectors are mutually orthogonal and uncorrelated and $(n - 1)$ have a zero mean, while one is proportional to the vector **1**. Each of these eigenvectors represents a distinct nature and degree of spatial autocorrelation. ESF introduces a subset of the eigenvectors as control variables in a regression model specification in order to capture its spatial stochastic component.

In linear regression, an ESF model specification can be expressed as

$$\mathbf{Y} = \mathbf{X}\boldsymbol{\beta} + \mathbf{E}_k \boldsymbol{\beta}_E + \boldsymbol{\varepsilon} \quad (4)$$

where **Y** denotes the dependent variable, **X** denotes a matrix of independent variables, $\mathbf{E}_k$ denotes a selected set of k eigenvectors selected from the n eigenvectors **E**, ($\boldsymbol{\beta}$, $\boldsymbol{\beta}_E$) denote parameters, and $\boldsymbol{\varepsilon}$ denotes random noise that is distributed $N(\mathbf{0}, \mathbf{I}\sigma^2)$. In this specification, $\mathbf{E}_k \boldsymbol{\beta}_E$ captures the spatial stochastic component in the dependent variable **Y**. Hence, the regression model does not suffer from complications attributable to spatial autocorrelation, which is likely to be observed in its residuals if the spatial stochastic component is not explicitly addressed.

The identification of $\mathbf{E}_k$ can be achieved through a stepwise procedure. Specifically, eigenvectors that minimize the level of spatial autocorrelation at each step can be selected. Intuitively, although this minimizing residual spatial autocorrelation criterion adheres to the notion of isolating spatial autocorrelation, it becomes computationally demanding as n increases. That is, in order to evaluate whether the addition of an eigenvector reduces spatial autocorrelation in residuals, the expected value and variance of Moran's I for the residuals needs to be recalculated repeatedly, which involves the inversion of large matrices.

This identification procedure can be assisted further by excluding irrelevant eigenvectors. The stepwise procedure can be conducted from a noticeably smaller set (i.e., a candidate set) instead of the entire set of eigenvectors, **E**. A candidate set can be demarcated based upon several criteria. First, eigenvectors that do not explain much spatial variation can be excluded. Second, eigenvectors that represent negative spatial autocorrelation can be excluded when variable **Y** displays positive spatial autocorrelation, and vice versa. This exclusion procedure can be assisted by the eigenvalues $\boldsymbol{\lambda}$, because λ_i is proportional to Moran's I value of a map that is a portrayal of $\mathbf{E}_i$ on the spatial tessellation from which **C** is created; Moran's $I = \lambda_i n/\mathbf{1}^T\mathbf{C}\mathbf{1}$. Hence, a candidate set is often constructed with a threshold minimum Moran's I value of 0.25,

which is related to approximately 5 % of the variation in a response variable being attributable to spatial autocorrelation."

3.3.3. Model validation

To further evaluate the model performance, the dataset was further split into training and test datasets. After being estimated based on the training dataset, and all the models were applied to the test dataset. Apart from the three types of regression models, a Bayesian model (i.e., the Bayesian linear regression model) and a popular machine learning model (i.e., the Random Forest regression model) were used to predict the test dataset for a broader comparison.

3.4. Implementation of analysis

In this study, the model selection, estimation, and validation were all implementable in *R*. Specifically, OLS model estimation, Moran's *I* testing, Lasso variable selection, MESS-SAR model estimation, and RES-ESF model estimation are supported by three *R* packages, named "stats", "spdep", "glmnet", "spatialreg", and "spmoran" respectively. And, prediction using Bayesian regression and Random Forest regression models were implemented via two *R* packages, named "bayesreg" and "randomForest" respectively. Besides, the bivariate Moran's *I* testing was implemented in GeoDa (http://geodacenter.github.io/index.html).

4. Results

In this section, spatial patterns of COVID-19 mortality rate are firstly explored, and lately, results of model selection and estimation are presented and discussed.

4.1 Spatial patterns of COVID-19 mortality rate

We first explored spatial patterns of COVID-19 mortality rate in comparison with non-COVID-19 mortality.

385 4.1.1 Spatial inequalities of COVID-19 mortality and non-COVID-19 mortality

386 The Gini coefficient for COVID-19 mortality rate and non-COVID-19 mortality rate across
387 England is 0.257 and 0.079 respectively. COVID-19 mortality rate has a much higher (about 3
388 times of) Gini coefficient than non-COVID-19 mortality rate. This indicates that the level of
389 spatial inequalities of COVID-19 mortality is higher than that of non-COVID-19 mortality in
390 England.

391 4.1.2 Spatial association of COVID-19 mortality and non-COVID-19 mortality

392 We performed the bivariate Moran's *I* tests of COVID-19 mortality rate and non-COVID-19
393 mortality rate. The global bivariate Moran's *I* value is 0.102 and the *p*-value is 0.001. The
394 global spatial association of COVID-19 mortality rate and non-COVID-19 mortality rate is
395 statistically significant and positive. The local bivariate Moran's *I* testing result is shown in
396 Figure 4. Figure 4 maps the clusters and outliers of COVID-19 mortality rate and non-COVID-
397 19 mortality rate across England. In Figure 4, all the clusters and outliers are statistically
398 significant at the 0.05 level. Clusters and outliers indicate the existence of positive and negative
399 local spatial association respectively. Specifically, 'High - High' and 'Low - Low' represent
400 two types of clusters; whilst 'Low - High' and 'High - Low' represent two types of outliers. In
401 Figure 4, 'High - High' means an area (LAD) with a high value of 'COVID-19 mortality rate'
402 is surrounded by areas (LADs) with a high value of 'non-COVID-19 mortality rate'; 'Low -
403 Low' means an area (LAD) with a low value of 'COVID-19 mortality rate' is surrounded by
404 areas (LADs) with a low value of 'non-COVID-19 mortality rate'； 'Low - High' means an
405 area (LAD) with a low value of 'COVID-19 mortality rate' is surrounded by areas (LADs) with
406 a high value of 'non-COVID-19 mortality rate' ; and 'High - Low' means an area (LAD) with
407 a high value of 'COVID-19 mortality rate' is surrounded by areas (LADs) with a low value of
408 'non-COVID-19 mortality rate'. For the COVID-19 prevention, areas deserving more
409 attentions are 'High - High' and 'High - Low' areas. Specifically, 'High - High' areas are

located around Sunderland, Liverpool, and Birmingham. ‘High - Low’ areas are located around London and Reading. Besides, ‘Low - Low’ areas are located in the southern England. Although global spatial association of COVID-19 mortality and non-COVID-19 mortality is positive, local spatial association of COVID-19 mortality and non-COVID-19 mortality is negative in some areas (e.g., ‘Low - High’ and ‘High - Low’ areas).

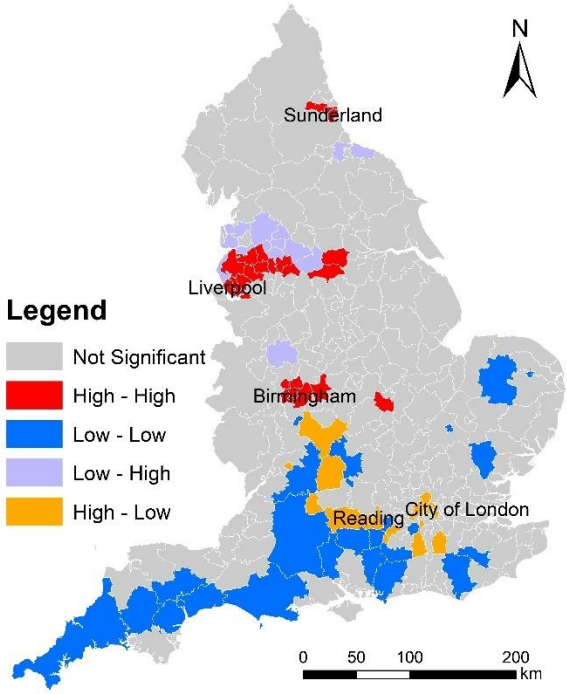

Figure 4. Clusters and outliers of COVID-19 mortality rate and non-COVID-19 mortality rate across England (March, April, and May 2020)

4.2 Model selection (spatial or non-spatial regression models)

4.2.1 Estimates of non-spatial regression model (OLS model)

First of all, non-spatial regression models (OLS models) were estimated based on 317 observations (317 LADs).

4.2.2 Estimates of spatial regression models (MESS and RES-ESF models)

Owing to the presence of significant spatial autocorrelation in the residuals of the OLS models estimated conventionally, we should select spatial models (e.g., MESS and RES-ESF models)

425 instead of non-spatial models (OLS models). Likewise, spatial models were estimated based
426 on 317 observations (317 LADs). Besides, in the estimation of ESF models, the eigenvectors
427 were selected by a stepwise method (see sub section 2.3.2). As aforementioned, threshold for
428 the eigenvalues is set to 0.25 (see sub section 2.3.2). As a result, 73 of 313 eigen-pairs were
429 extracted.

430 Table 3 lists the estimation results for the non-spatial and spatial models estimated, including
431 OLS, MESS-SAR, and RES-ESF models (N=317). The RES-ESF model outperforms the OLS
432 and MESS models owing to the highest R-squared value and the lowest Akaike information
433 criterion (AIC) value (R^2 = 0.797). Moreover, Moran's I test was used to test whether spatial
434 autocorrelation is present in the residuals of regression models estimated. As Table 3 shows,
435 statistically significant spatial autocorrelation is present in the OLS model but is not in the
436 MESS-SAR and RES-ESF models. This indicates that the replacing non-spatial regression
437 models (i.e., the OLS model) with spatial regression models (i.e., the MESS-SAR and RES-
438 ESF models) can reduce the potential bias owing to residual spatial autocorrelation.

439 Table 3 also shows the contributions of explanatory variables to spatial variations of COVID-
440 19 mortality rate. We discussed the contributions of explanatory variables according to the
441 estimation result of RE-ESF model (see Table 3). Expectedly, D_H (density of hospital) makes
442 a statistically significant contribution, and it is negatively related to COVID-19 mortality rate.
443 Therefore, areas with a low level of hospital accessibility are likely to suffer a high COVID-19
444 mortality rate. It is noted that some socioeconomic factors make statistically significant
445 contributions to spatial variations of COVID-19 mortality rate (see Table 3). Specifically, P_A
446 (percent of Asians), P_B (percent of Blacks), and UE_R (unemployment rate) are positively
447 related to COVID-19 mortality rate. This indicates that areas with a high percent of Asians, a
448 high percent of Blacks, or a high unemployment rate are likely to suffer a high COVID-19
449 mortality rate. More importantly, R_H (relative humidity) is statistically significantly and

450 negatively related to COVID-19 mortality rate; whilst R_AT (range of air temperature) is not
451 statistically significantly related to COVID-19 mortality rate.

452 **Table 3.** Estimation results for the non-spatial and spatial regression models (*N*=317)

Coefficient	OLS	MESS-SAR	RE-ESF
Intercept	587.326 ***	248.922 *	245.319 .
P_F	2.448	1.002	2.809 .
P_A	1.012 ***	0.782 ***	0.892 ***
P_B	2.758 ***	2.002 ***	2.58 ***
P_HIP	0.831 .	0.504	0.602
UE_R	5.943 ***	5.378 ***	4.807 ***
D_P	-1.612	-0.612	0.321
D_H	-0.099 .	-0.107 *	-0.08 *
AM_PM	-1.88	-1.984 .	-1.598
R_H	-8.521***	-3.715 **	-4.793 ***
R_AT	-0.795	1.512	3.852 .
Adjusted R^2	0.618	0.496	0.797
AIC	2858.418	2773.595	2776.084
Moran's *I* test for residuals	0.373***	0.032	-0.036

453 Note: '.', '*', '**', and '***' mean the *p*-values are below 0.1, 0.05, 0.01, and 0.001respectively.

454

455 4.2.3 Estimates of models after variable selection

456 Furthermore, to improve the model estimation, the Lasso technique is used to select the
457 influential explanatory variables. The optimal selection of explanatory variables are: P_A, P_B,
458 UE_R, D_H, and R_H. Table 4 lists the estimation results for the three models after the
459 explanatory variable selection (*N*=317). Expectedly, all the explanatory variables are
460 statistically significantly associated with the response in the three models. The RES-ESF model
461 consistently outperforms the OLS and MESS models owing to the highest *R*-squared value and
462 the lowest Akaike information criterion (AIC) value (R^2 = 0.793). Likewise, statistically
463 significant spatial autocorrelation is present in the OLS model but is not in the MESS-SAR and
464 RES-ESF models (see Table 4). Consistently, this indicates that the replacing non-spatial

regression models with spatial regression models can reduce the bias owing to residual spatial autocorrelation. Moreover, Table 5 shows correlations of residuals and explanatory variables in the models estimated. In Table 5, all the Pearson's correlation coefficients are extremely lowly valued, indicating no significant endogeneity of regressors exists. Besides, variance inflation factor (VIF) was used to detect multicollinearity in all the models estimated. In all the models estimated, the VIF values for all the independent variables (predictors) are below 5, indicating no serious multicollinearity exists in all these models estimated. This means all the all the independent variables (predictors) are not highly correlated to each other. Table 4 also shows the coefficients of the RE-ESF model is closer to the OLS model than the MESS-SAR model.

Table 4. Estimation results for the non-spatial and spatial regression models (N=317)

Coefficient	OLS	MESS-SAR	RE-ESF
Intercept	506.644 ***	199.041 **	390.149 ***
P_A	0.876 ***	0.708 ***	0.807 ***
P_B	2.155 ***	1.625 ***	2.522 ***
UE_R	6.756 ***	5.605 ***	4.971 ***
D_H	-0.124 *	-0.129 **	-0.122 ***
R_H	-6.029 ***	-2.366 **	-4.423 ***
Adjusted R^2	0.61	0.49	0.793
AIC	2859.7	2769.561	2784.813
Moran's *I* test for residuals	0.405***	0.046 .	-0.028

Note: '.', '*', '**', and '***' mean the *p*-values are below 0.1, 0.05, 0.01, and 0.001respectively.

Table 5. Correlations of residuals and explanatory variables in the models estimated

Pearson's correlation coefficient	Residuals		
	OLS	SAR-MESS	RE-ESF
P_A	-6.729×10^{-17}	5.826×10^{-18}	-2.270×10^{-13}
P_B	-7.968×10^{-17}	-3.181×10^{-17}	-1.580×10^{-13}
UE_R	-4.519×10^{-17}	-7.588×10^{-17}	-7.004×10^{-14}
D_H	-5.759×10^{-17}	-7.905×10^{-17}	1.139×10^{-13}
R_H	-9.482×10^{-16}	-5.200×10^{-16}	1.164×10^{-12}

4.2.4 Validation of models estimated

In this study, the dataset used was further split into the training and test datasets. Specifically, 20% of the cases are randomly selected as the test cases; whilst the remaining cases are selected as the training cases. Apart from OLS, MESS-SAR and RE-ESF models, Random Forest (RF) and Bayesian linear (BL) regression models were estimated based on the training dataset, and subsequently they are applied to the test data for a broader comparison. In this study, the Normalized Mean Absolute Error (NMAE) was used to measure the difference of prediction and real values after adjusting for scales. NMAE is the average of mean error normalized over the average of all the actual values. Table 6 shows the NMAE values for the predictions of COVID-19 mortality rate by different models. The RE-ESF model achieves the highest prediction accuracies with the lowest NMAE value. The prediction results indicate the RE-ESF model consistently outperforms the OLS and SAR-MESS models.

Table 6. Prediction accuracies of the regression models estimated

Model	**OLS**	**SAR-MESS**	**RE-ESF**	**BL**	**RF**
NMAE	0.267,808	0.368,653	0.267,177	0.267,18	0.284,087

4.3 Discussion

The RE-ESF model is likely to be the most proper model because 1) it outperforms the other two models in explaining spatial variations of COVID-19 mortality rate due to a higher R^2; 2) its coefficients are closer to the OLS model than the SAR-MESS model; 3) it substantially reduces the residual autocorrelation in comparison with the OLS model; and 4) it consistently outperforms the other models in predicting spatial variations of COVID-19 mortality rate due to a lower NMAE.

In the empirical study, some empirical findings were uncovered. Firstly, we uncovered that relative humidity is negatively related to COVID-19 mortality rate whilst $PM_{2.5}$ and air temperature measures are not significantly related. This finding is partly consistent with a previous study (e.g., Ma et al., 2020). In Wuhan, a positive association with COVID-19 daily death counts was observed for diurnal temperature range, but negative association for relative humidity (Ma et al., 2020). However, the negative association for relative humidity is consistent with our finding whilst the positive association for diurnal temperature range is not. More empirical studies are needed to examine the effects of temperature on COVID-19 daily death. Besides, a recent study found positive associations between particulate matter pollution ($PM_{2.5}$ and PM_{10}) and COVID-19 case fatality rate (CFR) in Chinese cities (Yao et al., 2020); whilst this study found no significant association between $PM_{2.5}$ and COVID-19 mortality rate. Secondly, we uncovered that percent of Asians and percent of Blacks is positively related to COVID-19 mortality rate. This is consistent with some previous findings on ethnical disparity in COVID-19 mortality (e.g., Aldridge et al., 2020; Holmes et al., 2020; Dyer, 2020; Pan et al., 2020). Thirdly, we uncovered that: unemployment rate is positively related to COVID-19 mortality rate; while density of hospital is negatively related to COVID-19 mortality rate. Consistent findings have been found to exist in France and China as discussed in the literature review section (Goutte et al., 2020; Ji et al., 2020). Particularly, combining Figure 4 and Figure 2b, we examined whether the hotspots of COVID-19 mortality rate and non-COVID-19 mortality rate are the areas with a lower level of access to hospital. As Figure 4 shows, high levels of COVID-19 mortality rate and high levels of non-COVID-19 mortality rate co-occur around Sunderland, Liverpool, and Birmingham. Those areas are likely to have a lower level of density of hospital as well (see Figure 2b). Healthcare resource allocation should prioritise those areas around Sunderland, Liverpool, and Birmingham.

Furthermore, the model estimation results reveal that spatial variations of COVID-19 mortality rate across England is mainly attributable to spatial variations of socioeconomical and environmental factors. This suggests that the reduction of socioeconomic disadvantage could potentially contribute to decrease in COVID-19 mortality risk across England. Socioeconomically disadvantaged areas are more likely to suffer a high risk of COVID-19 mortality. Governments and policy makers should consider how to reduce spatial disparities in COVID-19 mortality risk through decreasing socioeconomically disadvantaged population. Extremely disadvantaged areas should be given priority in policy making. Furthermore, we compared the non-spatial regression models (OLS models) and the spatial regression models (MESS-SAR and RES-ESF models) estimated in this study. The R^2 value of RES-ESF model estimated are higher than those of OLS and MESS-SAR models. Therefore, RES-ESF model is empirically found to outperform OLS and MESS-SAR models in this study. Applications of spatial regression models are likely to better model spatial variations of COVID-19 mortality rate across England. Moreover, RES-ESF model is highly recommended to be applied to a variety of applications in urban or regional studies.

In this study, $PM_{2.5}$ is not reported to be significantly associated with COVID-19 mortality whilst the significant association is reported in studies on some other regions (e.g., Yao et al., 2020; Gupta et al., 2020; Coker et al., 2020). One possible reason is: compared to the cities or areas in the previous studies (Yao et al., 2020; Gupta et al., 2020; Coker et al., 2020), England has a lower level of $PM_{2.5}$, thereby spatial variations of $PM_{2.5}$ between English LADs is likely to be smaller than those between the cities or areas in the previous studies. Additionally, we have taken account of other air pollutants (e.g., NO_2 and SO_2) as other potential environmental factors in more model estimations like Table 3 and 4. Defra also offers 1x1 km gridded annual mean NO_2 and SO_2 data for 2019 (https://uk-air.defra.gov.uk/data/pcm-data). Like $PM_{2.5}$, NO_2

548 and SO_2 are not statistically significantly related to COVID-19 mortality rate after adjusting
549 for the other socioeconomic and environmental factors.

550 **5. Conclusion**

551 In this study, we examined the spatial patterns of COVID-19 mortality rate in relation to
552 socioeconomic and environmental factors across England. Two newly developed specifications
553 of spatial regression models were established successfully to estimate COVID-19 mortality
554 rate. The level of spatial inequalities of COVID-19 mortality is higher than that of non-COVID-
555 19 mortality in England. Although global spatial association of COVID-19 mortality and non-
556 COVID-19 mortality is positive, local spatial association of COVID-19 mortality and non-
557 COVID-19 mortality is negative in some areas. The model estimated indicate that 1) relative
558 humidity is negatively related to COVID-19 mortality rate; 2) hospital accessibility is
559 negatively related to COVID-19 mortality rate; and 3) percent of Asians, percent of Blacks,
560 and unemployment rate are positively related to COVID-19 mortality rate. Moreover, the RES-
561 ESF model estimated outperforms the MESS-SAR model in modelling spatial variations of
562 COVID-19 mortality rate across England.

563 However, there are some limitations in this study. Firstly, in this study, we take no account of
564 behavioural factors, such as alcohol consumption and sugar drinks intake, due to the lack of
565 data. Human health is found to be affected by behavioural factors (e.g., dietary patterns, diet
566 quality, sugary drinks intake, fruits and vegetable intake, alcohol and tobacco consumption,
567 sleep duration, sleep quality, etc.) (Richter et al. 2012; Patel et al. 2013). Secondly, as the
568 poverty data used is for 2014, the time gap between poverty data and other data is relatively
569 large. The existence of this time gap might have a potential influence on the model estimation
570 in this study. Besides, the poverty data is available for 2014, whether the spatial variations of
571 poverty are proportional to those in continuous years needs to be empirically validated. Thirdly,

the data used reflect the registered deaths caused by COVID-19, but they might completely reflect the actual deaths caused by COVID-19. On the one hand, the presence of false positives is likely to over-estimate the number of deaths owing to COVID-19. On the other hand, some deaths caused by COVID-19 are likely to be recognised as non-COVID-19 deaths especially in the earlier stage of pandemic when testing capacity is low.

In the future, we will improve this study by addressing those limitations. Firstly, we will attempt to acquire data on behavioural characteristics from questionnaire-based surveys in collaboration with National Health Service (NHS) England. The acquired data will be used to measure behavioural factors. Secondly, the study needs to be repeated once some research data (e.g., poverty data) is updated in the future. The results would be compared with the those in this paper to discuss the influence of time gap in some data on the model estimation results.

CRediT authorship contribution statement

Yeran Sun: Conceptualization, Data curation, Formal analysis, Writing - review & editing. Xuke Hu: Conceptualization, Writing - review & editing. Jing Xie: Writing - review & editing.

Ethical approval and consent to participate

Not applicable.

Consent for publication

Not applicable.

Availability of supporting data

The datasets used and/or analyzed during the current study are available from the websites.

Funding

Not applicable.

Declaration of interest statement The authors declare that they have no conflict of interest

Acknowledgments We would like to thank anonymous reviewers for taking the time and effort to review the manuscript.

References:

Adekunle, I.A., Onanuga, A., Wahab, O. and Akinola, O.O., 2020. Modelling spatial variations of coronavirus disease (COVID-19) in Africa. *Science of The Total Environment*, p.138998.

Aldridge, R.W., Lewer, D., Katikireddi, S.V., Mathur, R., Pathak, N., Burns, R., Fragaszy, E.B., Johnson, A.M., Devakumar, D., Abubakar, I. and Hayward, A., 2020. Black, Asian and Minority Ethnic groups in England are at increased risk of death from COVID-19: indirect standardisation of NHS mortality data. *Wellcome Open Research*, *5*(88), p.88.

Barreca, A.I. and Shimshack, J.P., 2012. Absolute humidity, temperature, and influenza mortality: 30 years of county-level evidence from the United States. *American journal of epidemiology*, *176*(suppl_7), pp.S114-S122.

Beelen, R., Raaschou-Nielsen, O., Stafoggia, M., Andersen, Z.J., Weinmayr, G., Hoffmann, B., Wolf, K., Samoli, E., Fischer, P., Nieuwenhuijsen, M. and Vineis, P., 2014. Effects of long-term exposure to air pollution on natural-cause mortality: an analysis of 22 European cohorts within the multicentre ESCAPE project. *The Lancet*, *383*(9919), pp.785-795.

Chi, G. and Zhu, J., 2008. Spatial regression models for demographic analysis. *Population Research and Policy Review*, 27(1), pp.17-42.

Chun, Y. 2014. Analyzing space–time crime incidents using eigenvector spatial filtering: an application to vehicle burglary. *Geographical Analysis*, 46 (2): pp.165-184.

Chun, Y., Griffith, D. A., Lee, M., and Sinha, P. 2016. Eigenvector Selection with Stepwise Regression Techniques to Construct Eigenvector Spatial Filters. J*ournal of Geographical Systems*, 18 (1): 67–85.

Coker, E.S., Cavalli, L., Fabrizi, E., Guastella, G., Lippo, E., Parisi, M.L., Pontarollo, N., Rizzati, M., Varacca, A. and Vergalli, S., 2020. The effects of air pollution on COVID-19 related mortality in northern Italy. *Environmental and Resource Economics*, 76(4), pp.611-634.

Cordes, J. and Castro, M.C., 2020. Spatial analysis of COVID-19 clusters and contextual factors in New York City. *Spatial and Spatio-temporal Epidemiology*, p.100355.

Danon, L., Brooks-Pollock, E., Bailey, M. and Keeling, M.J., 2020. A spatial model of CoVID-19 transmission in England and Wales: early spread and peak timing. *MedRxiv*.

Desjardins, M.R., Hohl, A. and Delmelle, E.M., 2020. Rapid surveillance of COVID-19 in the United States using a prospective space-time scan statistic: Detecting and evaluating emerging clusters. *Applied Geography*, p.102202.

Di, Q., Dai, L., Wang, Y., Zanobetti, A., Choirat, C., Schwartz, J.D. and Dominici, F., 2017. Association of short-term exposure to air pollution with mortality in older adults. *Jama*, *318*(24), pp.2446-2456.

Dyer, O., 2020. Covid-19: Black people and other minorities are hardest hit in US. BMJ, 369, m1483.

Engebretsen, S. and Bohlin, J., 2019. Statistical predictions with glmnet. *Clinical epigenetics*, 11(1), pp.1-3.

Friedman, J., Hastie, T. and Tibshirani, R., 2010. Regularization paths for generalized linear models via coordinate descent. *Journal of statistical software*, 33(1), p.1.

Gatto, M., Bertuzzo, E., Mari, L., Miccoli, S., Carraro, L., Casagrandi, R. and Rinaldo, A., 2020. Spread and dynamics of the COVID-19 epidemic in Italy: Effects of emergency containment measures. *Proceedings of the National Academy of Sciences*, *117*(19), pp.10484-10491.

Gasparrini, A., Guo, Y., Hashizume, M., Lavigne, E., Zanobetti, A., Schwartz, J., Tobias, A., Tong, S., Rocklöv, J., Forsberg, B. and Leone, M., 2015. Mortality risk attributable to high and low ambient temperature: a multicountry observational study. *The Lancet*, *386*(9991), pp.369-375.

Guliyev, H., 2020. Determining the spatial effects of COVID-19 using the spatial panel data model. *Spatial statistics*, p.100443.

644 Guo, Y., Gasparrini, A., Armstrong, B., Li, S., Tawatsupa, B., Tobias, A., Lavigne, E., Coelho,
645 M.D.S.Z.S., Leone, M., Pan, X. and Tong, S., 2014. Global variation in the effects of ambient
646 temperature on mortality: a systematic evaluation. *Epidemiology (Cambridge, Mass.)*, *25*(6), p.781.

647 Halonen, J.I., Hansell, A.L., Gulliver, J., Morley, D., Blangiardo, M., Fecht, D., Toledano, M.B.,
648 Beevers, S.D., Anderson, H.R., Kelly, F.J. and Tonne, C., 2015. Road traffic noise is associated with
649 increased cardiovascular morbidity and mortality and all-cause mortality in London. *European heart*
650 *journal*, *36*(39), pp.2653-2661.

651 Héritier, H., Vienneau, D., Foraster, M., Eze, I.C., Schaffner, E., Thiesse, L., Rudzik, F., Habermacher,
652 M., Köpfli, M., Pieren, R. and Brink, M., 2017. Transportation noise exposure and cardiovascular
653 mortality: a nationwide cohort study from Switzerland. *European journal of epidemiology*, *32*(4),
654 pp.307-315.

655 Helbich, M., and Arsanjani, J.J. 2015. Spatial eigenvector filtering for spatiotemporal crime mapping
656 and spatial crime analysis. *Cartography and Geographic Information Science*, 42 (2): 134-148.

657 Hoek, G., Krishnan, R.M., Beelen, R., Peters, A., Ostro, B., Brunekreef, B. and Kaufman, J.D., 2013. Long-
658 term air pollution exposure and cardio-respiratory mortality: a review. *Environmental health*, *12*(1), p.43.

659 Hohl, A., Delmelle, E., Desjardins, M. and Lan, Y., 2020. Daily surveillance of COVID-19 using the
660 prospective space-time scan statistic in the United States. *Spatial and Spatio-temporal Epidemiology*,
661 p.100354.

662 Holmes, L., Enwere, M., Williams, J., Ogundele, B., Chavan, P., Piccoli, T., Chinacherem, C., Comeaux,
663 C., Pelaez, L., Okundaye, O. and Stalnaker, L., 2020. Black–White Risk Differentials in COVID-19
664 (SARS-COV2) Transmission, Mortality and Case Fatality in the United States: Translational
665 Epidemiologic Perspective and Challenges. *International journal of environmental research and public*
666 *health*, *17*(12), p.4322.

667 Huang, R., Liu, M. and Ding, Y., 2020. Spatial-temporal distribution of COVID-19 in China and its
668 prediction: A data-driven modeling analysis. *The Journal of Infection in Developing Countries*, *14*(03),
669 pp.246-253.

Getis, A., and Ord, J.K. (1992). The Analysis of Spatial Association by Use of Distance Statistics. *Geographical Analysis*, 24, 189-206.

Griffith, D. A. 2003. Spatial autocorrelation and spatial filtering: gaining understanding through theory and scientific visualization. Springer Science & Business Media.

Goutte, S., Péran, T. and Porcher, T., 2020. The role of economic structural factors in determining pandemic mortality rates: evidence from the COVID-19 outbreak in France. *Research in International Business and Finance*, *54*, p.101281.

Gupta, A., Bherwani, H., Gautam, S., Anjum, S., Musugu, K., Kumar, N., Anshul, A. and Kumar, R., 2020. Air pollution aggravating COVID-19 lethality? Exploration in Asian cities using statistical models. *Environment, Development and Sustainability*, pp.1-10.

Ji, Y., Ma, Z., Peppelenbosch, M.P. and Pan, Q., 2020. Potential association between COVID-19 mortality and health-care resource availability. *The Lancet Global Health*, *8*(4), p.e480.

Kosidou, K., Dalman, C., Lundberg, M., Hallqvist, J., Isacsson, G., & Magnusson, C. (2011). Socioeconomic status and risk of psychological distress and depression in the Stockholm Public Health Cohort: a population-based study. *Journal of affective disorders*, *134*(1-3), 160-167.

Lelieveld, J., Evans, J.S., Fnais, M., Giannadaki, D. and Pozzer, A., 2015. The contribution of outdoor air pollution sources to premature mortality on a global scale. *Nature*, *525*(7569), pp.367-371.

LeSage J.P., & Pace, R.K. (2007). A matrix exponential spatial specification. *Journal of Econometrics*, 140, 190-214.

LeSage J.P., & Pace, R.K. (2009). *Introduction to Spatial Econometrics*. CRC Press, Chapter 9.

Lin, X., 2010. Identifying peer effects in student academic achievement by spatial autoregressive models with group unobservables. *Journal of Labor Economics*, 28(4), pp.825-860.

Mollalo, A., Vahedi, B. and Rivera, K.M., 2020. GIS-based spatial modeling of COVID-19 incidence rate in the continental United States. *Science of The Total Environment*, p.138884.

694 Ma, Y., Zhao, Y., Liu, J., He, X., Wang, B., Fu, S., Yan, J., Niu, J., Zhou, J. and Luo, B., 2020. Effects
695 of temperature variation and humidity on the death of COVID-19 in Wuhan, China. *Science of The*
696 *Total Environment*, p.138226.

697 Met Office; Hollis, D.; McCarthy, M.; Kendon, M.; Legg, T.; Simpson, I. (2020): HadUK-Grid Gridded
698 Climate Observations on a 1km grid over the UK, v1.0.2.1 (1862-2019). Centre for Environmental Data
699 Analysis, date of citation. https://catalogue.ceda.ac.uk/uuid/89908dfcb97b4a28976df806b4818639
700 Moran, P.A. (1950). Notes on continuous stochastic phenomena. *Biometrika*, 37(1/2), 17-23.

701 Murakami, D. and Griffith, D.A., 2015. Random effects specifications in eigenvector spatial filtering:
702 a simulation study. *Journal of Geographical Systems*, *17*(4), pp.311-331.

703 Murakami, D. and Griffith, D.A. 2019. Eigenvector spatial filtering for large data sets: fixed and random
704 effects approaches. *Geographical Analysis*, 51 (1), 23-49.

705 Nobles, J., Weintraub, M.R., & Adler, N.E. (2013). Subjective socioeconomic status and health:
706 relationships reconsidered. *Social Science & Medicine*, 82, 58-66.

707 Ou, C.Q., Jun, Y.A.N.G., Ou, Q.Q., Liu, H.Z., Lin, G.Z., Chen, P.Y., Jun, Q.I.A.N. and Guo, Y.M.,
708 2014. The impact of relative humidity and atmospheric pressure on mortality in Guangzhou,
709 China. *Biomedical and Environmental Sciences*, *27*(12), pp.917-925.

710 Pan, D., Sze, S., Minhas, J.S., Bangash, M.N., Pareek, N., Divall, P., Williams, C.M., Oggioni, M.R.,
711 Squire, I.B., Nellums, L.B. and Hanif, W., 2020. The impact of ethnicity on clinical outcomes in
712 COVID-19: A systematic review. *EClinicalMedicine*, p.100404.

713 Patel, C.J., Rehkopf, D.H., Leppert, J.T., Bortz, W.M., Cullen, M.R., Chertow, G.M., & Ioannidis, J.P.
714 (2013). Systematic evaluation of environmental and behavioural factors associated with all-cause
715 mortality in the United States National Health and Nutrition Examination Survey. *International journal*
716 *of epidemiology*, *42*(6), 1795-1810.

717 Präg, P., Mills, M.C., & Wittek, R. (2016). Subjective socioeconomic status and health in cross-national
718 comparison. *Social Science & Medicine*, 149, 84-92.

719 Pujari, B.S. and Shekatkar, S.M., 2020. Multi-city modeling of epidemics using spatial networks:
720 Application to 2019-nCov (COVID-19) coronavirus in India. *medRxiv*.

721 Richter, M., Moor, I., & van Lenthe, F.J. (2012). Explaining socioeconomic differences in adolescent
722 self-rated health: the contribution of material, psychosocial and behavioural factors. *Journal of*
723 *Epidemiology & Community Health*, 66(8), 691-697.

724 Tibshirani, R., 1996. Regression shrinkage and selection via the lasso. *Journal of the Royal Statistical*
725 *Society: Series B (Methodological)*, 58(1), pp.267-288.

726 Velásquez, R.M.A. and Lara, J.V.M., 2020. Forecast and evaluation of COVID-19 spreading in USA
727 with Reduced-space Gaussian process regression. *Chaos, Solitons & Fractals*, p.109924.

728 Wheeler, B.W., Lovell, R., Higgins, S.L., White, M.P., Alcock, I., Osborne, N.J., Husk, K., Sabel, C.E.,
729 & Depledge, M.H. (2015). Beyond greenspace: an ecological study of population general health and
730 indicators of natural environment type and quality. *International journal of health geographics*, *14*(1),
731 17.

732 Yao, Y., Pan, J., Wang, W., Liu, Z., Kan, H., Qiu, Y., Meng, X. and Wang, W., 2020. Association of
733 particulate matter pollution and case fatality rate of COVID-19 in 49 Chinese cities. *Science of the Total*
734 *Environment*, p.140396.

735 Zheng, R., Xu, Y., Wang, W., Ning, G. and Bi, Y., 2020. Spatial transmission of COVID-19 via public
736 and private transportation in China. *Travel Medicine and Infectious Disease*.

737